British Journal of Mathematics & Computer Science
17(1): 1-26, 2016, Article no.BJMCS.26359
ISSN: 2231-0851

SCIENCEDOMAIN *international*
www.sciencedomain.org

Formulation of Time Dependent Bloch NMR Equations for Computational Analyses of Nano Particles in Porous Media

A. A. Adeleke[1*]

[1]Department of Physics and Engineering Physics, University of Saskatchewan, Saskatoon, Canada.

Author's contribution

The sole author designed, analyzed and interpreted and prepared the manuscript.

Article Information

DOI: 10.9734/BJMCS/2016/26359
Editor(s):
(1) Dariusz Jacek Jakóbczak, Chair of Computer Science and Management in this Department, Technical University of Koszalin, Poland.
Reviewers:
(1) Eugene Mananga, The City University of New York, USA.
(2) Bharat Raj Jaiswal, AKS University, Satna, India.
Complete Peer review History: http://sciencedomain.org/review-history/14872

Original Research Article

Received: 13th April 2016
Accepted: 24th May 2016
Published: 1st June 2016

Abstract

Nuclear Magnetic Resonance (NMR) has been very useful in the study of pore size distribution of porous materials and in molecular recognition. Important properties of the porous media have been shown to be very much dependent on the T_1 and T_2 relaxation times. The NMR transverse magnetization carries information on the pores' properties. This has been demonstrated by many experiments on porous media but analytical expressions showing the direct relationships between the pore features and the NMR parameters have been quite scarce in literature. In this study, formulation of time dependent Bloch NMR equation for computational analyses of nano particles in porous media has been presented. Since the nano particle is expected to be imaged in a nano-porous medium, we apply the transformation that makes the NMR transverse magnetization $M_y(t)$ expressible in term of $M_y(p)$ with porosity $p(t)$. Two new parameters which validate the transformation are properly defined in terms of the porosity, T_1 and T_2 relaxation parameters. The results obtained in this study can have applications in functional magnetic resonance imaging (fMRI), Petroleum exploration and well design, geological engineering and could be a frontier towards a very robust way of describing porousity and permeability in systems transporting particles of specific shape and form.

Keywords: Bloch NMR equations; porosity; transverse magnetization; nano particles; porous media.

**Corresponding author: E-mail: adelekeabayo@gmail.com;*

1 Introduction

The study of viscous flow through permeable media has attracted substantial interest in science, engineering, and technology. The flow through permeable media takes place generally in geophysical and bio-mechanical systems and also has many engineering applications, such as, flow in fixed beds, petroleum industry, hydrology etc. Due to its broad areas of applications in science, engineering and industries, many different theoretical and experimental models have been used for describing the viscous flow past and through bulk materials or porous bodies [1,2]. With porous structured in the above mentioned areas, the structure of porous lamina must be considered and analyzed from all point of views. For analytical study of the fluid flows within porous structured bodies, so called porous media, the two terms: Porosity and permeability play significant and vital role. The porosity is defined as the ratio of voids' volume to that of the volume of the material. Theoretically, it seems that if the material has more pores (voids), it will allow the fluid to pass through it easily, but actually it is not so and could be understood through the permeability which is defined as the easiness or ability (inter connectivity of pores) of the material to allow the fluids to pass through it [1-3]. Various methods and models have been written to describe this phenomenon of flow through materials characterized by pores, but very few of them really perform well when it comes to giving quantitave information with high resolution. Magnetic resonance imaging (MRI) uses a powerful magnetic field along with radio waves and a computer to produce highly detailed pictures of virtually all internal structures of matter. The result enables physicians to examine parts of the body quickly and in a more detailed way. MRI enables physicians to see through and identify diseases in a way that are not possible with other techniques.

The principal ideas behind magnetic resonance are common to both electron spin resonance (ESR) and nuclear magnetic resonance (NMR), but there are differences in the magnitudes and signs of the magnetic interactions involved, which of course lead to divergences in the experimental techniques being implemented. In principle, all nuclei with odd mass number possess the property of spin; the spin angular momentum vector which is commonly denoted by $\boldsymbol{I}\hbar$, measured in unit of ħ, and ħ is the Planck's constant divided by 2π. In a macroscopic assembly of protons subjected to an external field B(x), we expect to find some protons with α spin and some with β spin [4].

Magnetic Resonance Imaging technique for nano-particle in biological system is a multiphysics process involving diverse physical domains such as magnetic fields and fluid dynamics. It is also a multiscale investigative process suitable for materials ranging from mini dimensions of the arteries to micro dimensions of the capillaries and micro particles down to the nano dimensions of single domain super paramagnetic particles [5,6]. For example, the protein structure could be taken from the crystallographic measurements, though Visual Molecular Dynamics (VMD) simulations are often used to relax the crystal structure to a more plausible conformation for specific physiological conditions. To resolve even longer time scales, the protein and lipid structures could be modelled as continuum regions delimited by hard wall boundaries, and characterized electrically by an average permittivity and static charge distribution. Mean while, MRI, through correct application of NMR flow equations can achieve even more when we model signals from each NMR-sensitive nuclei in term of their transverse magnetization. Thus, we can formulate and study the movement of micro or nano materials through pores of comparable sizes, with set of coupled differential equations known as the Bloch's equations with relatively small computer cost. Fig. 1 below shows the simulation of the movement of Deoxyribonucleic Acid (DNA) by VMD. The whole process, of course could be conceptualized as a nanorobot transiting through a Si_3N_4 membrane, which is made of pores at the nanoscale level. Such simulation is computationally expensive and time consuming, while similar information could be deduced by simulation of magnetic resonance (MR) signals from the DNA and the Si_3N_4 nuclei.

Evidently there is neither a complete modelling framework nor a single software package for simulating the entire process. This would require the integration of multiparticle simulation, molecular simulation, continuum-based models, stochastic methods and nanomechanics [7,8]. Nonetheless, critical physical parameters are captured by the simplified model of the fundamental Bloch NMR flow equation specifically adopted for porous medium. The analytical solutions to the Bloch equation can provide fundamental

computational tools which can stimulate interest for future research at the molecular and atomic scales for conceptualization, characterization, development of nano particles either in the form of nanorobots or nano machines [9,10].

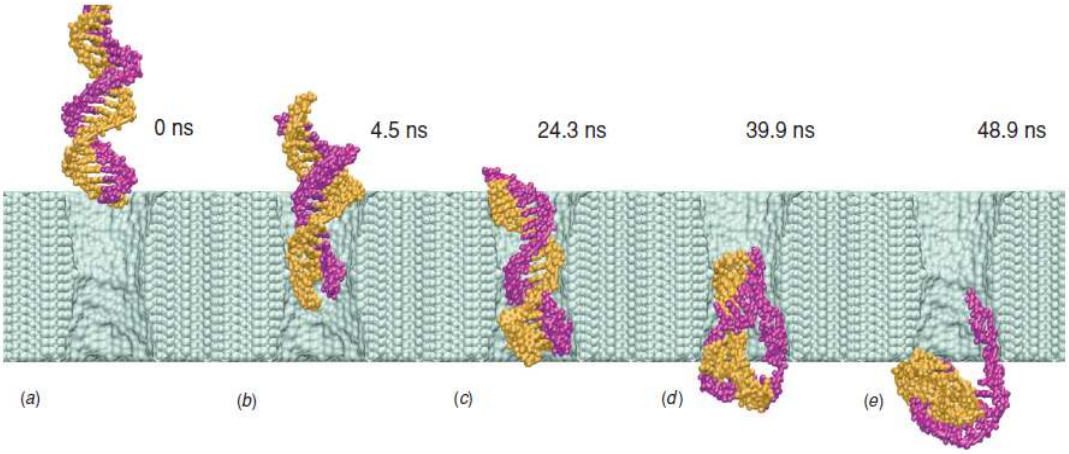

Fig. 1. VMD and NAMD simulation of DNA translocation through a nanopore in a Si_3N_4 membrane
(a) Beginning of the simulation. (b) The moment when the terminal Watson–Crick base pair is split at the narrowest part of the pore. (c) A moment during the time interval of 8 ns that DNA spends in the conformation shown without moving. (d) The moment when DNA exits the pore while one base at the DNA end remains firmly attached to the surface of the nanopore. (e) End of the simulation, when most of the DNA has left the pore and the ionic current has returned to the open pore level [7]

2 Mathematical Formulation of Bloch NMR Equations

The phenomenon of Nuclear Magnetic Resonance which is the underlying physics behind Magnetic Resonance Imaging is known to be governed by the Bloch NMR flow equations. These differential equations in their coupled form relate magnetization to the applied radio frequency, gradient and static magnetic field. It is a known fact that the body and many other materials are made up of various NMR-sensitive nuclei, whose spatial and time variation are captured by the Bloch equations. If we consider a bulk magnetic moment **M** (also known as the magnetization vector) of large assembly of spins at a certain temperature, they could either be electron or nuclear spin. With the help of an external field, $N_\propto$ of them are in the α spin state and, N_β of them are in the β state [4], then the macroscopic magnetization vector's behaviour under any condition is given by the following set of equations in the various Cartesian coordinate:

$$\frac{dM_x}{dt} = \frac{\partial M_x}{\partial t} + v\frac{\partial M_x}{\partial x} = -\frac{M_x}{T_2} \tag{1}$$

$$\frac{dM_y}{dt} = \frac{\partial M_y}{\partial t} + v\frac{\partial M_y}{\partial x} = \gamma M_z B_1(x) - \frac{M_y}{T_2} \tag{2}$$

$$\frac{dM_z}{dt} = \frac{\partial M_z}{\partial t} + v\frac{\partial M_z}{\partial x} = -\gamma M_z B_1(x) - \frac{M_0 - M_z}{T_1} \tag{3}$$

The above systems of equations (1,2,3) were used to derive a generalized partial differential equation (PDE) that can be used for the analysis of any system composed of NMR-sensitive material by imposing suitable boundary conditions [11-13]. The fundamental NMR time dependent second order differential equation which is applicable to any fluid flow problem at any given time [11-14] is thus given by:

$$v^2\frac{\partial^2 M_y}{\partial x^2}+2v\frac{\partial^2 M_y}{\partial x\partial t}+vT_0\frac{\partial M_y}{\partial x}+T_0\frac{\partial M_y}{\partial t}+\frac{\partial^2 M_y}{\partial t^2}+\left(T_g+\gamma^2B_1^2(x,t)\right)M_y=\frac{M_0}{T_1}\gamma B_1(x,t) \quad (4)$$

Where M_y is the transverse magnetization also known as the Magnetic Resonance (MR) signal, $T_0=\frac{1}{T_1}+\frac{1}{T_2}$, $T_g=\frac{1}{T_1+T_2}$. T_1 is the spin-lattice, T_2 is the spin-spin relaxation time, γ is the gyromagnetic ratio, $B_1(x,t)$ is the external magnetic field and the function $\frac{M_0}{T_1}\gamma B_1(x,t)$ is the forcing term.

3 Formulation of Bloch Equation for Steady Flow in Porous Media

In a study done by Storm, Arnold J, et al. [15], it was opined that the dynamics of the DNA through the Si_3N_4 was in fact not dependent on spatial distance and does not change appreciably over a large x for say a long time. From the knowledge of the analysis of PDE, it is thus safe to equate every $\frac{\partial^n}{\partial x^n}$ term to zero for such situation. Invoking this condition on equation (4), it becomes:

$$\frac{d^2M_y}{dt^2}+T_0\frac{dM_y}{dt}+\left(T_g+\gamma^2B_1^2(t)\right)M_y=\frac{M_0\gamma B_1(t)}{T_1} \quad (5)$$

In this study, we will solve the time dependent modified Bloch NMR flow equation given in equation (5) using Hermite series method of solution. As a matter of fact, what comes to mind is that there are other methods of solution that as well can be used to derive the solution to equation (5), some of which are given in [12,13,15]. However, we have chosen to present our solution using series method because the addition operation is more computationally cheaper than many of the methods of solution that have been provided. Equation (5) can be reduced based on three reasonable initial conditions [3,11,12,14]:

1. $M_0\neq M_z$; a situation which holds good in general and in particular when radio frequency $B_1(t)$ field is strong say of the order of 1.0 Gauss or more.
2. Before entering the signal detector coil, nanoparticle bolus has magnetization $M_x=0$, $M_y=0$.
3. $B_1(t)$ is large; $B_1(t)$ >> 1 Gauss or more so that M_y of the nanoparticle bolus changes appreciably from M_o i.e when $\gamma^2B_1^2(t)\ll\frac{1}{T_1T_2}$.

So that equation (5) reduces to:

$$\frac{d^2M_y}{dt^2}+T_0\frac{dM_y}{dt}+T_gM_y=\frac{M_0\gamma B_1(t)}{T_1} \quad (6)$$

Equation (6) can be significantly useful to analytically model the phenomenological dynamics of a nano particle moving through a biological porous material. Since the nano particle is expected to be imaged in a nano-porous medium (blood flow), we apply the transformation [3,11,16-18] that will make $M_y(t)$ expressible in term of $M_y(p)$. This condition transforms $M_y(t)$ into a porous medium with porosity $p(t)$, such that

$$\frac{dM_y}{dt}=\frac{dM_y}{dp}\frac{dp}{dt} \quad (7)$$

Using the product rule, the second derivative can be derived:

$$\frac{d^2M_y}{dt^2} = \frac{d^2M_y}{dp^2}\left(\frac{dp}{dt}\right)^2 + \frac{dM_y}{dp}\frac{d^2p}{dt^2} \tag{8}$$

Using equation (7) and (8), equation (6) becomes:

$$\frac{d^2M_y}{dp^2}\left(\frac{dp}{dt}\right)^2 + \frac{dM_y}{dp}\frac{d^2p}{dt^2} + T_0\frac{dM_y}{dp}\frac{dp}{dt} + \left(T_g + \gamma^2B_1^2(t)\right)M_y = \frac{M_0\gamma B_1(t)}{T_1} \tag{9}$$

Equation (9) can be written in the form

$$\frac{d^2M_y}{dp^2} + A\frac{dM_y}{dp} + a^2M_y = a^2T_2M_0\gamma B_1(t) \tag{10}$$

Where

$$A = \left[\frac{\left(\frac{d^2p}{dt^2}\right)}{\left(\frac{dp}{dt}\right)^2} + T_0\frac{\left(\frac{dp}{dt}\right)}{\left(\frac{dp}{dt}\right)^2}\right] \tag{11}$$

$$a^2 = \frac{T_g}{\left(\frac{dp}{dt}\right)^2} \tag{12}$$

For equation (10) to be valid, parameter a^2 must be any positive integer and A must be a constant. $p(t)$ is the porosity. For the purpose of obtaining fundamental (semi classical and quantum mechanical) information about the variation of porosity with time for fluid dynamics evaluation in porous media, we consider a case where A=0, equation (10) becomes:

$$\frac{d^2M_y}{dp^2} + a^2M_y = a^2T_2M_0\gamma B_1(t) \tag{13}$$

Equation (13) allows us to discuss the dynamics of the NMR system quantum mechanically if we define the radio frequency field as:

$$\omega_1 = \gamma B_1(t) = p^2M_y(p) \ll \frac{1}{\sqrt{T_1T_2}}$$

Equation (13) can be solved for the case of maximum signal where the equilibrium magnetization $M_0 = 0$ and other cases where $M_0 \neq 0$.

4 Solution of the Bloch NMR Flow Equations in Porous Media

At maximum signal **(** $M_0 = 0$ **),** equation (13) becomes:

$$\frac{d^2 M_y}{dp^2} + a^2 M_y = 0 \tag{14}$$

The generalization solution to equation (14) when $a_1 = 0, a_0 \neq 0,$ and all $a_{2n-1} = 0$ is given by:

$$M_{y1}(p) = (-1)^n c_0 \sum_{n=0}^{\infty} \frac{a^{2n} p^{2n}}{(2n)!} \tag{15}$$

When **(** $\boldsymbol{a_1 \neq 0}, n = 2n-1, a_0 \neq 0$ **),** the generalization solution to equation (14) is given by:

$$M_{y2}(p) = (-1)^n c_1 \sum_{n=1}^{\infty} \frac{p^{2n-1} a^{2(n-1)}}{(2n-1)!} \tag{16}$$

Equations (15) and (16) are the two fundamental solutions of equation (14) so that by linear combination of solution, the general solution to equation (14) using the method of series solution becomes:

$$M_y(p) = (-1)^n c_0 \sum_{n=0}^{\infty} \frac{a^{2n} p^{2n}}{(2n)!} + \quad (-1)^n c_1 \sum_{n=1}^{\infty} \frac{p^{2n-1} a^{2(n-1)}}{(2n-1)!} \tag{17}$$

Where C_0 and C_1 are coefficients that are not zero.

The porosity p(t) suitable for equation (17) is obtained by solving the branch of differential equation (11) for the case where A = 0. Thus, the porosity was found [3,19-21] to be:

$$p = p(t) = p_0 \exp(-T_0 t) \tag{18}$$

Solution to equation (13) for a physical case where the equilibrium magnetization $M_0 \neq 0$ leads to an equation similar in form to Schrödinger wave equation for a simple harmonic oscillator and the Hermite differential equation as below:

$$\begin{aligned} &\Psi''(x) + \left(\frac{2mE}{\hbar^2} - \frac{mkx^2}{\hbar^2} \right) \Psi(x) = 0 \\ &Y''(x) - 2xY'(x) + 2nY(x) = 0 \\ &\frac{d^2 M_y}{dp^2} + a^2 \left(1 - M_0 T_2 p^2\right) M_y = 0 \end{aligned} \tag{19}$$

The solution to equation (19) is

$$M_{yn}(p) = H_n(p)\exp\left(-\frac{p^2}{2}\right) \tag{20}$$

Where

$$H_n(p) = \sum_{n=0}^{\infty} C_n \left(T_2 M_o\right)^{\frac{1}{4}} a^{\frac{1}{2}} p(t) \tag{21}$$

and

$$2n+1 = \frac{a}{\sqrt{T_2 M_0}} \quad \text{Where n=0, 1, 2, 3…} \tag{21a}$$

Equation (20) becomes

$$M_{yn}(p) = \sum_{n=0}^{\infty} C_n \left(T_2 M_o\right)^{\frac{1}{4}} a^{\frac{1}{2}} p(t)\exp\left(-\frac{p^2}{2}\right) \tag{22}$$

Where the recursion formula is given as

$$C_{n+2} = \left(\frac{n(1+U)-(U+Q)}{(n+2)(n+1)}\right) C_n$$

and $Q = \left(\frac{a}{\sqrt{T_2 M_0}} - U^2\right)$, $U = (T_2 M_0)^{\frac{1}{4}} a^{\frac{1}{2}}$

Equation (22) is the solution to the time dependent Bloch NMR flow equation (13) using the Hermite series solution method, when the equilibrium magnetization$M_0 \neq 0$. We also derived a single valued solution of the Bloch NMR equation as:

$$M_y(p) = D_1 \exp\left(\frac{\left(T_2 M_o\right)^{\frac{1}{2}} a p^2}{2}\right) \tag{23}$$

Where D_1 is a constant that could be the intrinsic magnetization of the MRI system.

The general solution of equation (11) when $A \neq 0$ is [3].

$$p(t) = \frac{1}{A}\left\{\ln\left[\exp(T_0 t)\right] - \ln\left[(K_2 \exp(T_0 t) - A\right]\right\} + c_2 \tag{24}$$

For cases where A was assumed to be zero, the porosity of the system was obtained using equation (18) and equation (24) for cases where A is assumed not to be equal to zero.

5 Variation of $M_y(p)$ with p(t) and t (s) for Varying Values of n when $M_o=0$ and A=0

Analysis of equation (17) shows that the porosity of a nano porous material varies exponentially with NMR signal and relaxation parameter T_o. This implies that at the molecular level, the porosity decreases at an exponential rate as time of measurement increases, starting from the intrinsic maximum porosity of the material at time t=0 i.e. p(t=0)=p_0 where p_0 was chosen to be unity as shown in Figs. 2-12. A possible explanation for this decay is because of the free induction decay experienced by the MR signal (Transverse Magnetization) when the equilibrium magnetization M_o have been assumed to be equal to zero. This implies that the total magnetic field B1 applied to the nanoporous material is totally converted into magnetic force that excites the proton near the pore of the material and when the B_1 field is withdrawn, the magnetic force come down to zero freely through an exponential decay that starts from the maximum excitation that the B1 field was able to give to the nano porous material's pore.

A 3D plot of $M_y(p)$, p(t) and time t(s) was made to visualize the behaviour of the MR signal (Transverse Magnetization) as the pore open or closes with time, which signifies the time or point of initiation of the nanoparticle's movement through the nanopores and a point when the movement has been completed by varying the number of harmonics (which corresponds to the number of protons in the pore been imaged) present in the MR signal. It was observed that the wave signifying the nature of the movement of the pore was more predominant and significant when the quantum number of harmonics n=1, more so, porosity was consistent which invariably implies the motion of the nanoparticle through the nanopore at that instant and at a main field of 1.5 Tesla is consistent. The contour graph was used to simulate contrast of the MR signal as the porosity changes with time i.e. p(t) was plotted against t(s), and the contrast shown represents the intensity of the MR signal (Transverse Magnetization). In other words, the Legend shows the distribution of MR signal strength as porosity changes with time. This goes a long way to give handful information on clarity and stratification pattern of MR signals, as the pore open and closes with time, for varying quantum number of harmonics, and it was observed that a clearer contrast and layer (strata) was formed when the number of harmonics n=1,2,….,10. This tells us that the MR signal carries better information about protons for which n=1 and above. Hence for the second time it can be concluded that the MR signal carries more information about intrinsic proton of nanopores, relative to which the imaging of a nanoparticle is made. Also a characteristics pattern-less nature of the contour plot for n=0 implies that no MR signal emerges in the absence of excitation of proton. Finally, for n=2 and above, the behaviour of the MR signal alternates with alternating odd and even value of quantum harmonic number 'n'.

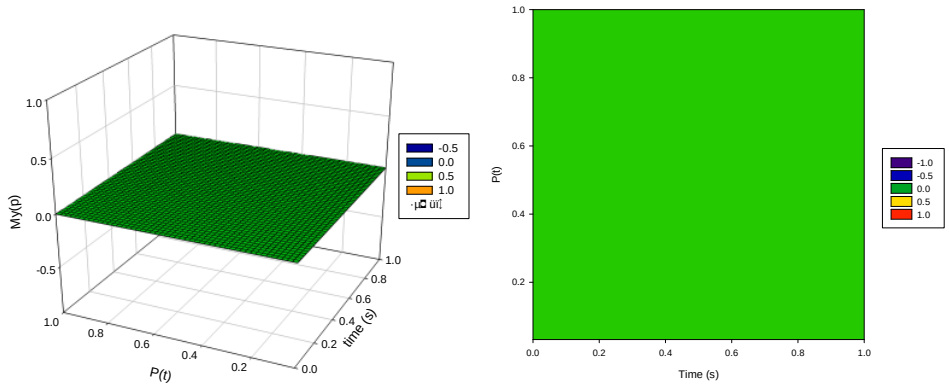

(a) (b)

Fig. 2. (a) 3D graph of equation (17) for $M_0=0$, A=0, n=0 (b) Contour graph of equation (17) for $M_o=0$, A=0, n=0

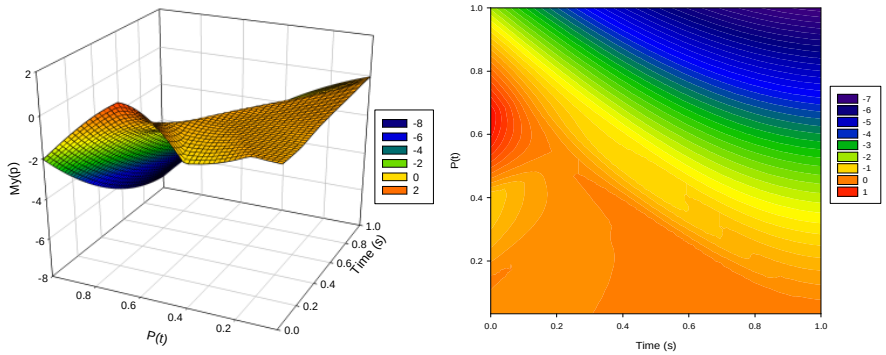

(a) (b)

Fig. 3. (a) 3D graph of equation (17) for M_o=0, A=0, n=1 (b) Contour graph of equation (17) for M_o=0, A=0, n=1

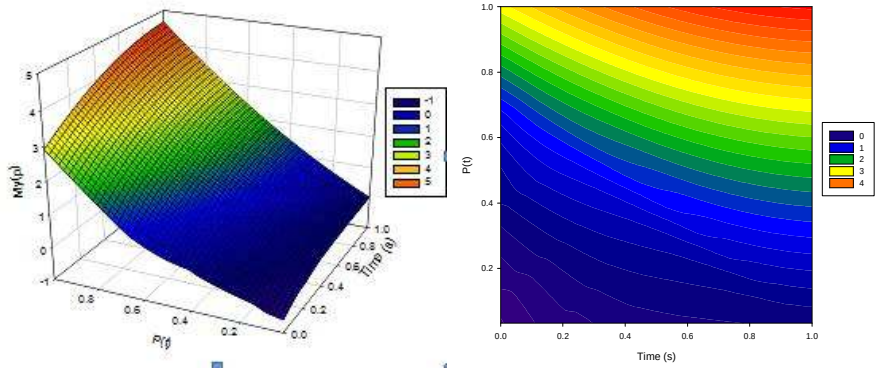

(a) (b)

Fig. 4. (a) 3D graph of equation (17) for Mo=0, A=0, n=2 (b) Contour graph of equation (17) for Mo=0, A=0, n=2

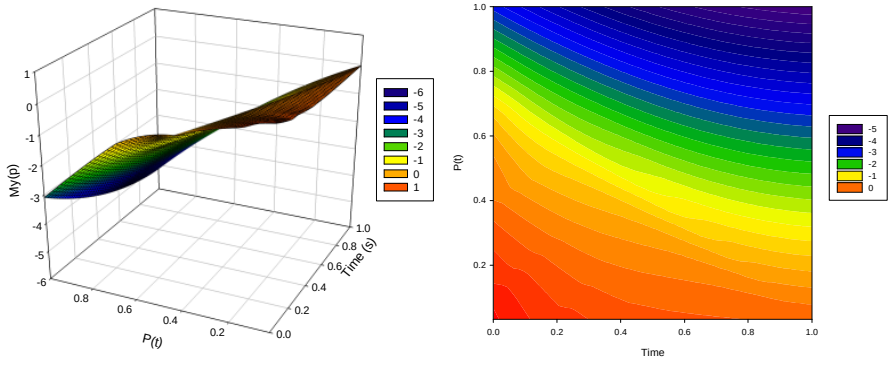

(a) (b)

Fig. 5. (a) 3D graph of equation (17) for Mo=0, A=0, n=3 (b) Contour graph of equation (17) for Mo=0, A=0, n=3

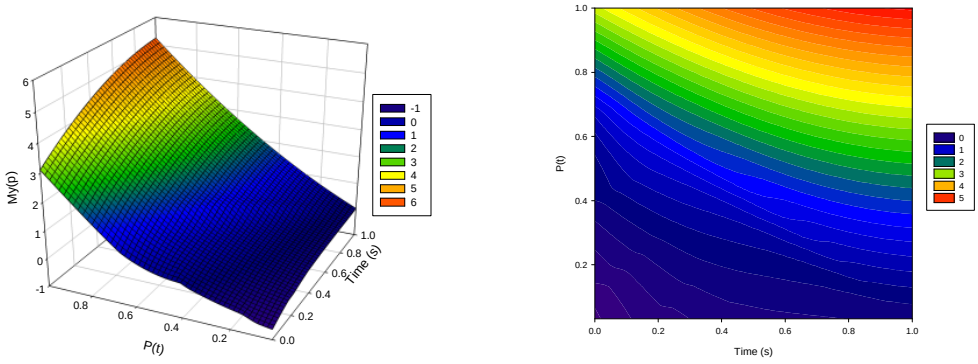

(a) (b)

Fig. 6. (a) 3D graph of equation (17) for Mo=0, A=0, n=4 (b) Contour graph of equation (17) for Mo=0, A=0, n=4

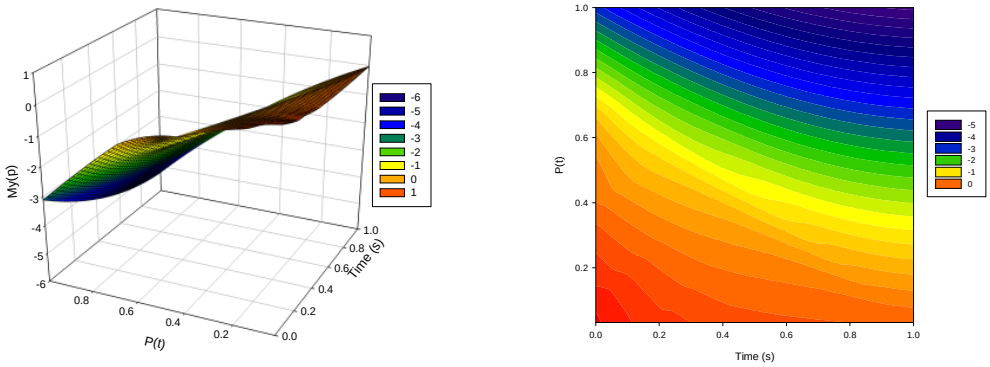

(a) (b)

Fig. 7. (a) 3D graph of equation (17) for Mo=0, A=0, n=5 (b) Contour graph of equation (17) for Mo=0, A=0, n=5

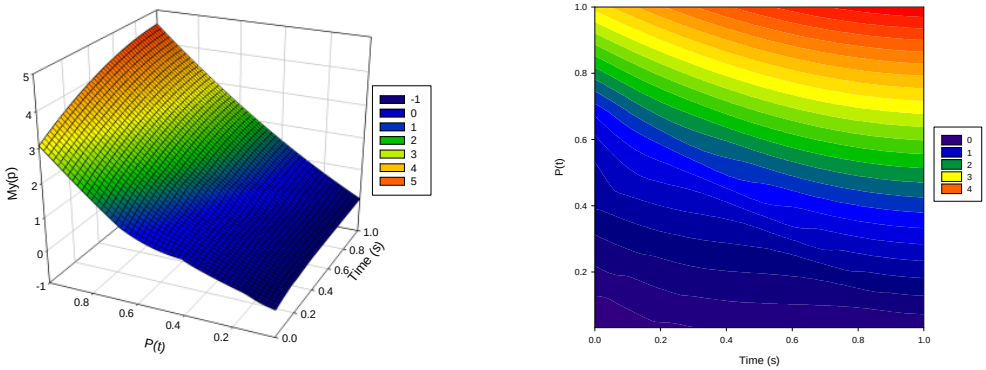

(a) (b)

Fig. 8. (a) 3D graph of equation (17) for Mo=0, A=0, n=6 (b) Contour graph of equation (17) for Mo=0, A=0, n=6

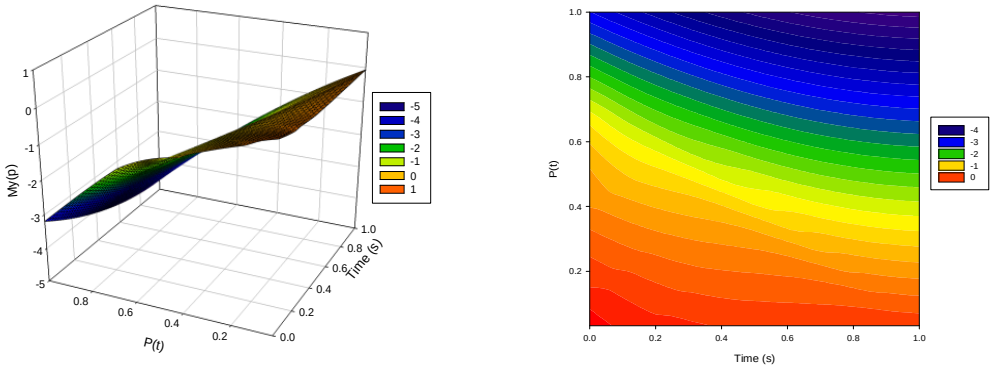

(a) (b)

Fig. 9. (a) 3D graph of equation (17) for Mo=0, A=0, n=7 (b) Contour graph of equation (17) for Mo=0, A=0, n=7

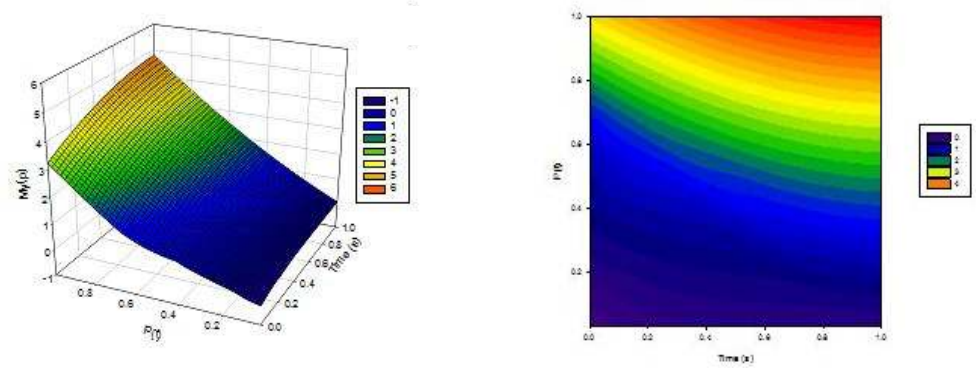

(a) (b)

Fig. 10. (a) 3D graph of equation (17) for Mo=0, A=0, n=8 (b) Contour graph of equation (17) for Mo=0, A=0, n=8

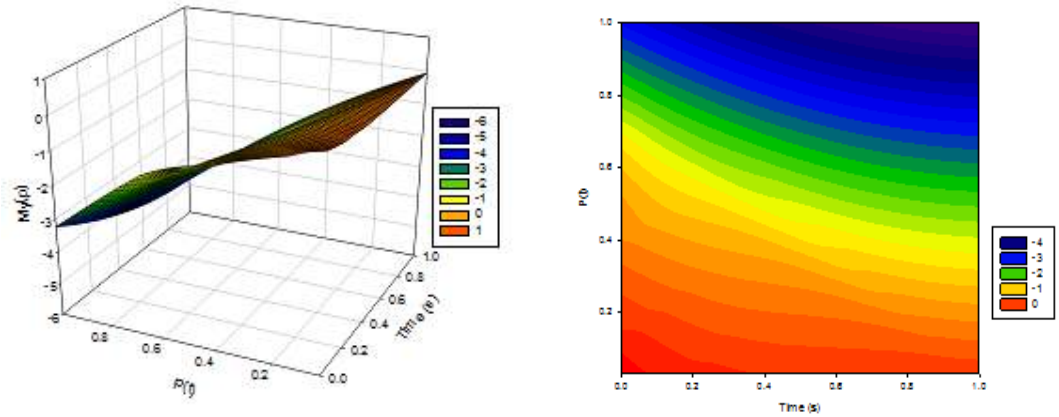

(a) (b)

Fig. 11. (a) 3D graph of equation (17) for Mo=0, A=0, n=9 (b) Contour graph of equation (17) for Mo=0, A=0, n=9

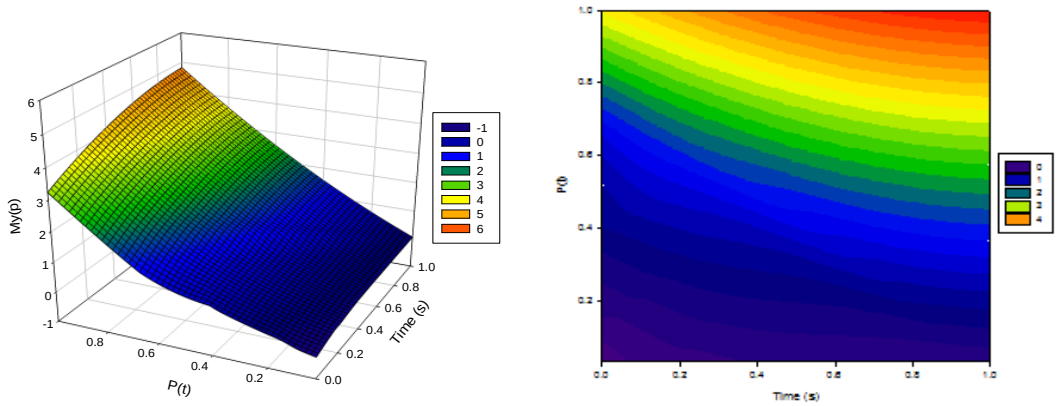

(a) (b)

Fig. 12. (a) 3D graph of equation (17) for Mo=0, A=0, n=10 (b) Contour graph of equation (17) for Mo=0, A=0, n=10

6 Variation of My(p) with p(t) and t(s) for Varying Values of n and a when $M_0 \neq 0$

From a thorough characterization and vivid observation of Figs. 13-17 that describe equation (22), it was observed that for n=0 and A=1, there was no MR signal (Transverse Magnetization). This also shows that the transverse magnetization does not pick up as pore of nanoporous material opens or closes. Under this consideration, the porosity is not a pure exponential function of time, but a mixture of natural logarithm and exponential function of both the spin-lattice and spin-spin relaxation time. It was observed that as 'n' increases to 1, the behaviour of the MR signal changes and indicates that the pore is either opening or closing with time. The magnitude of MR signal increases slightly with time up to 0.6 sec after which the rate increases linearly. As 'n' increases to 2, the MR signal starts from a peak value for a single proton and decrease slowly with time up to 0.6 sec, where the signal start to decrease linearly. The MR signal maintain this trend as the pore opens with time until n=4 where the MR signal exhibit a full wave behaviour after a short 'blankness' for about 0.3 sec. As the pore opens towards its intrinsic porosity, the MR signal rapidly and linearly increases. The MR signal maintain the same trend even for n=5.

As 'A' increases to 2, the behaviour of MR signal generally is similar to that observed when A was equal to 1. Nonetheless, it is worthy of note that in some specific cases, some particular behaviours were observable, that include the fact that the full wave behaviour of MR signal slightly become less significant and that the magnitude of the MR signal become greater than is observable when A=1. More so, it was observed that as 'A' increases, the maximum porosity of the pore found on a nanoporous material decreases. This implies that as 'A' increases, the maximum diameter with which the pore open up decreases. This is evident in the solution given by equation (24), which gives no expression, about the surface's maximum porosity (otherwise known as the porous material's intrinsic porosity).

On a more broad term, it can be concluded based on the behaviour of these graphs that increase or decrease in the value of A only increases or decreases the maximum porosity observed respectively, which in turn increases the MR signal and make it behave similar to analysis given above as time of observation increases. Though there were exceptional cases where the MR signal decreases as in the case where quantum number 'n' equal 2 and 3.

(a)

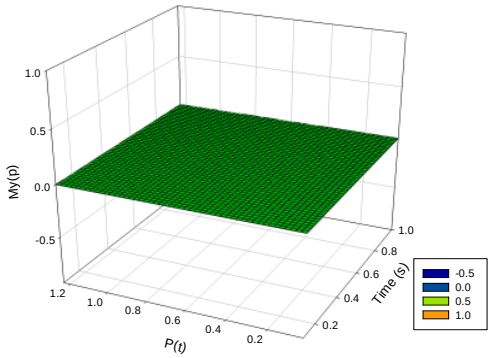
3D Graph of My(p), P(t) and t(s) for n=0, A=1
My(p)
P(t)
Time (s)
-0.5
0.0
0.5
1.0

(b)

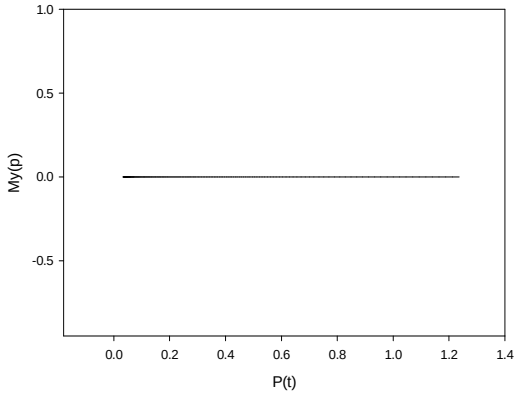
2D Graph of My(p) and P(t) for n=0, A=1
My(p)
P(t)

(c)

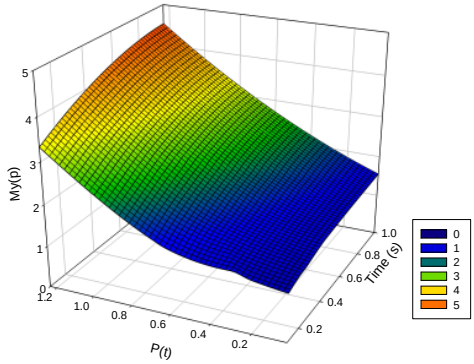
3D Graph of My(p), P(t) and t(s) for n=1, A=1
My(p)
P(t)
Time (s)
0
1
2
3
4
5

(d)

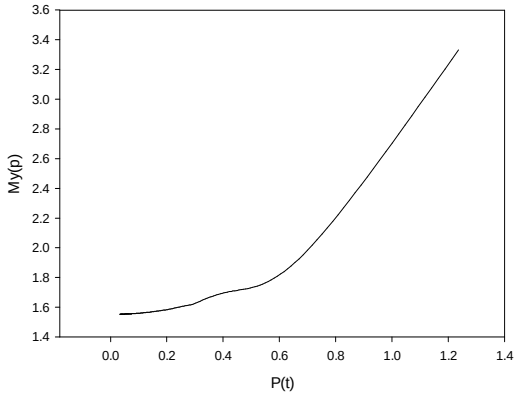
2D Graph of My(p) and P(t) for n=1, A=1
My(p)
P(t)

(e)

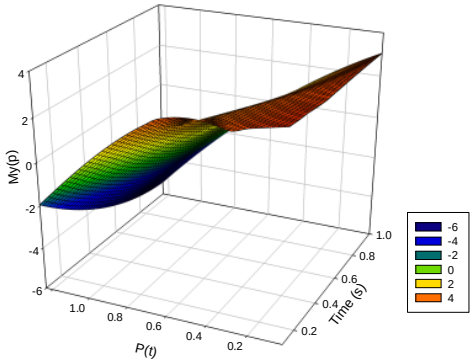
3D Graph of My(p), P(t) and t(s) for n=2, A=1
My(p)
P(t)
Time (s)
-6
-4
-2
0
2
4

(f)

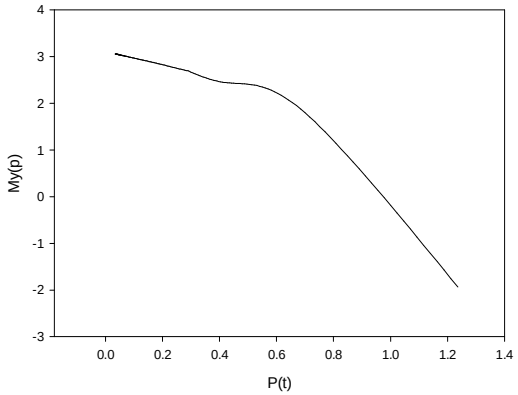
2D Graph of My(p) and P(t) for n=2, A=1
My(p)
P(t)

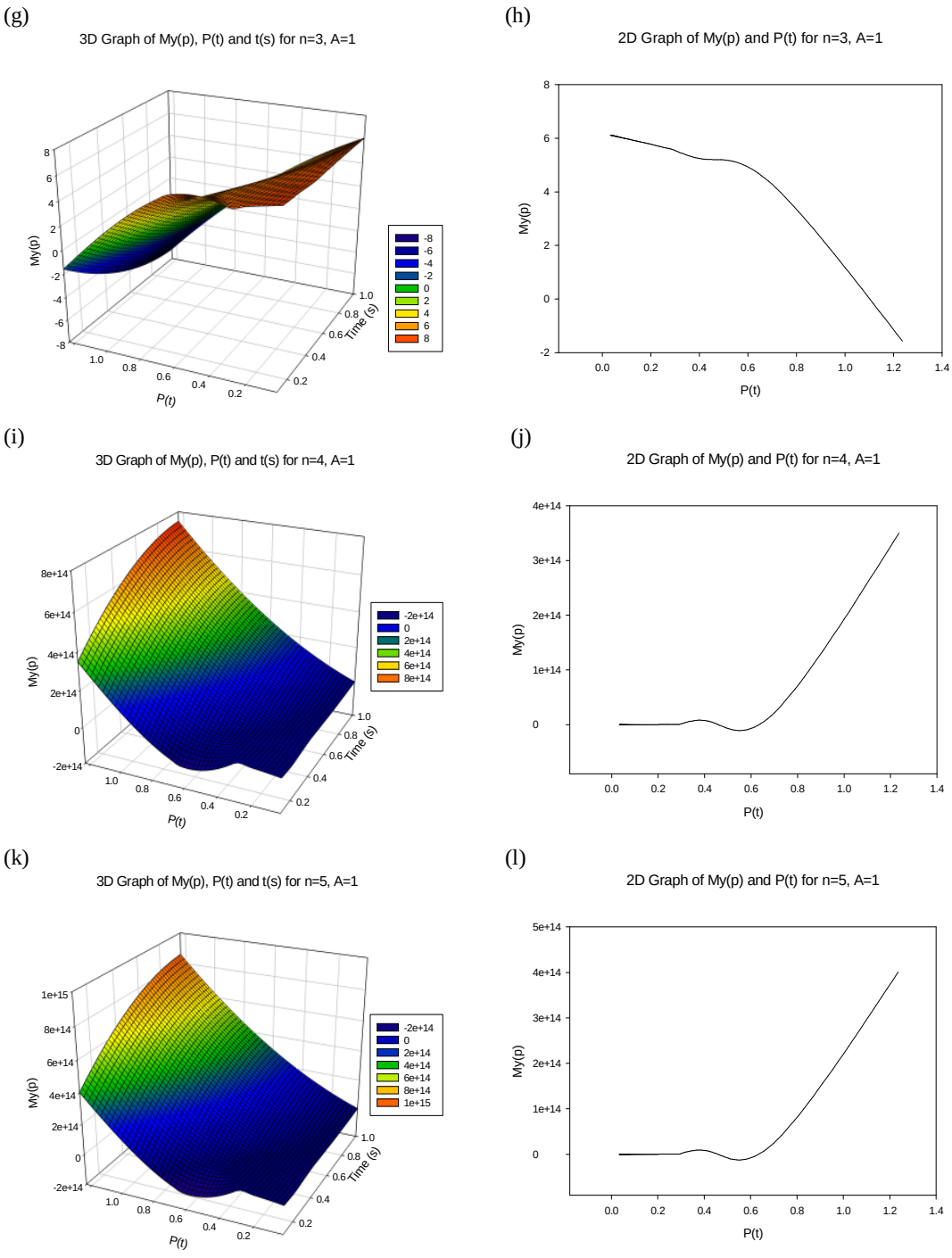

Fig. 13. 3D & 2D graph of equation (22) for A=1, Mo≠0, (a) n=0, (b) n=0, (c) n=1, (d) n=1, (e) n=2, (f) n=2, (g) n=3, (h) n=3, (i) n=4, (j) n=4, (k) n=5, (l) n=5, for 3D and 2D respectively

(a)

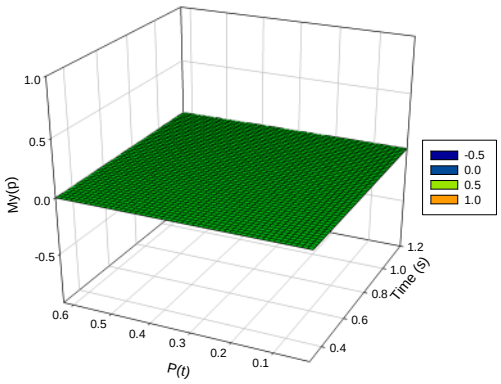
3D Graph of My(p), P(t) and t(s) for n=0, A=2
My(p)
P(t)
Time (s)
-0.5
0.0
0.5
1.0

(b)

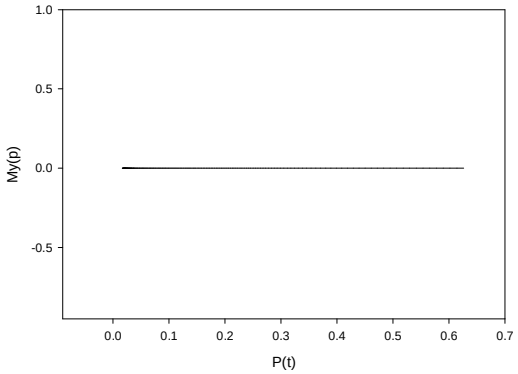
2D Graph of My(p) and P(t) for n=0, A=2
My(p)
P(t)

(c)

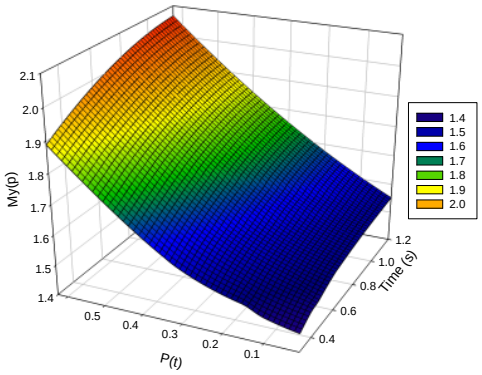
3D Graph of My(p), P(t) and t(s) for n=1, A=2
My(p)
P(t)
Time (s)
1.4
1.5
1.6
1.7
1.8
1.9
2.0

(d)

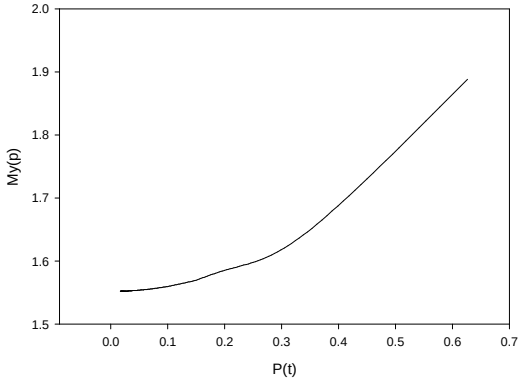
2D Graph of My(p) and P(t) for n=1, A=2
My(p)
P(t)

(e)

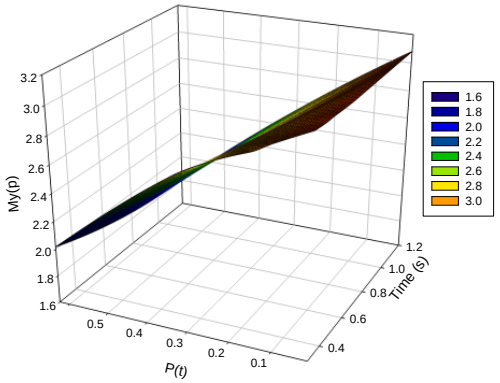
3D Graph of My(p), P(t) and t(s) for n=2, A=2
My(p)
P(t)
Time (s)
1.6
1.8
2.0
2.2
2.4
2.6
2.8
3.0

(f)

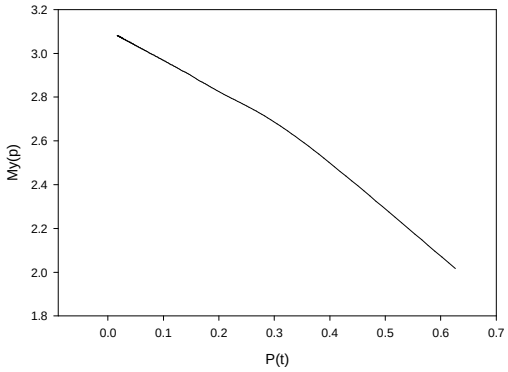
2D Graph of My(p) and P(t) for n=2, A=2
My(p)
P(t)

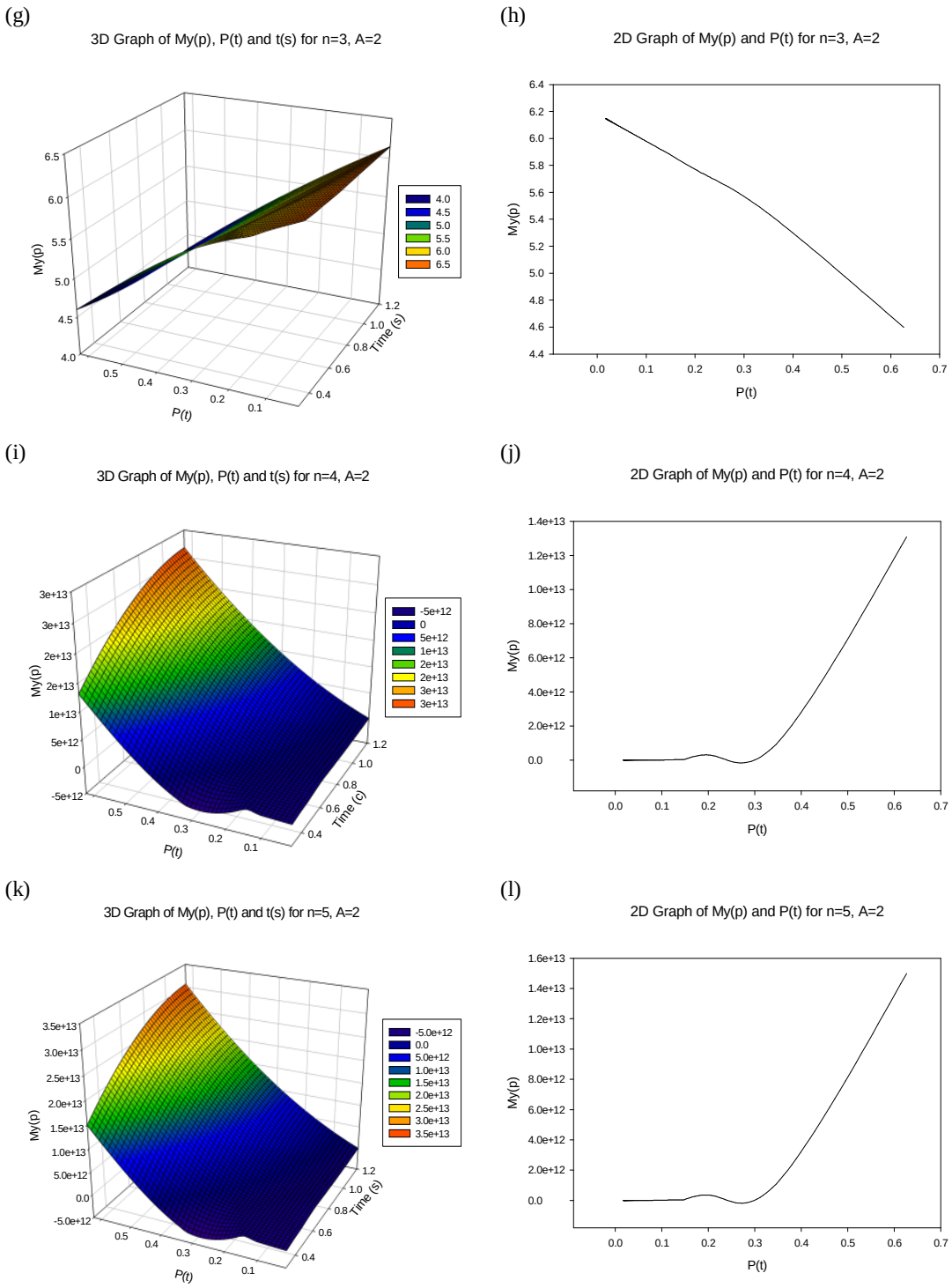

Fig. 14. 3 D & 2 D graph of equation (22) for A=2, Mo≠0, (a) n=0(b) n=0, (c) n=1, (d) n=1, (e) n=2, (f) n=2, (g) n=3, (h) n=3, (i) n=4, (j) n=4, (k) n=5, (l) n=5, for 3D and 2D respectively

(a)

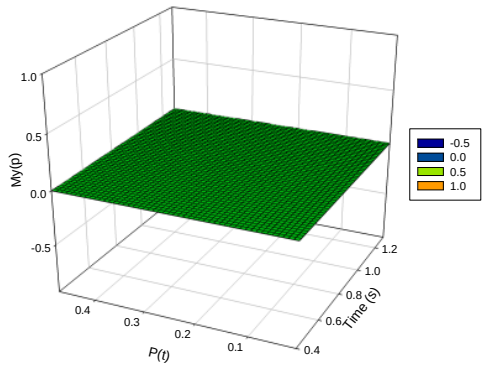
3D Graph of My(p), P(t) and t(s) for n=0, A=3
My(p)
P(t)
Time (s)
-0.5
0.0
0.5
1.0

(b)

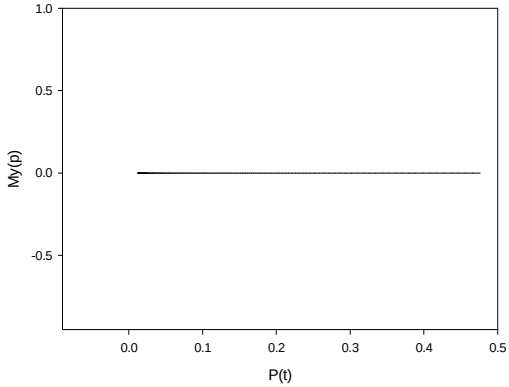
2D Graph of My(p) and P(t) for n=0, A=3
My(p)
P(t)

(c)

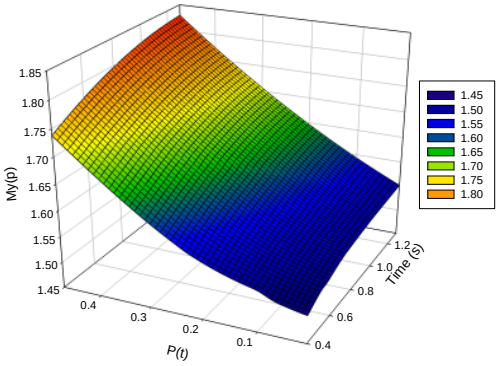
3D Graph of My(p), P(t) and t(s) for n=1, A=3
My(p)
P(t)
Time (s)
1.45
1.50
1.55
1.60
1.65
1.70
1.75
1.80

(d)

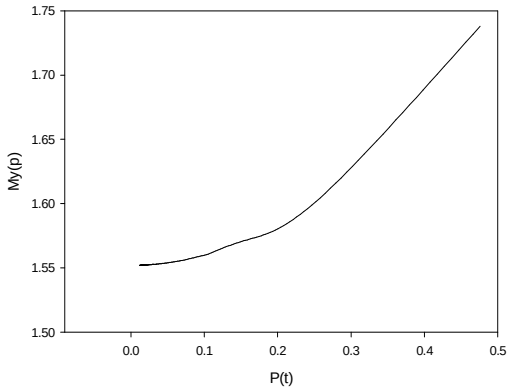
2D Graph of My(p) and P(t) for n=1, A=3
My(p)
P(t)

(e)

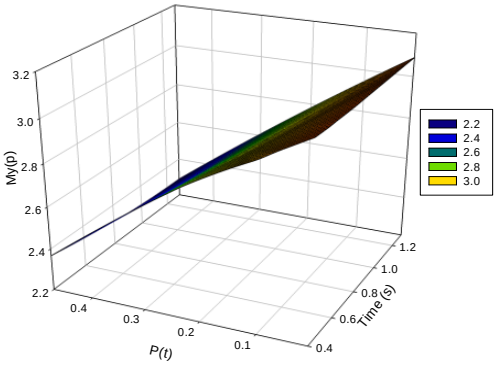
3D Graph of My(p), P(t) and t(s) for n=2, A=3
My(p)
P(t)
Time (s)
2.2
2.4
2.6
2.8
3.0

(f)

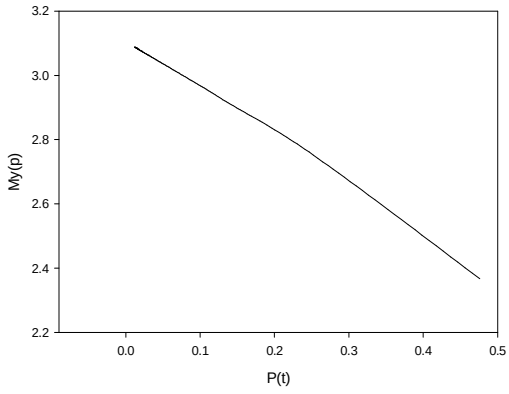
2D Graph of My(p), P(t) and t(s) for n=2, A=3
My(p)
P(t)

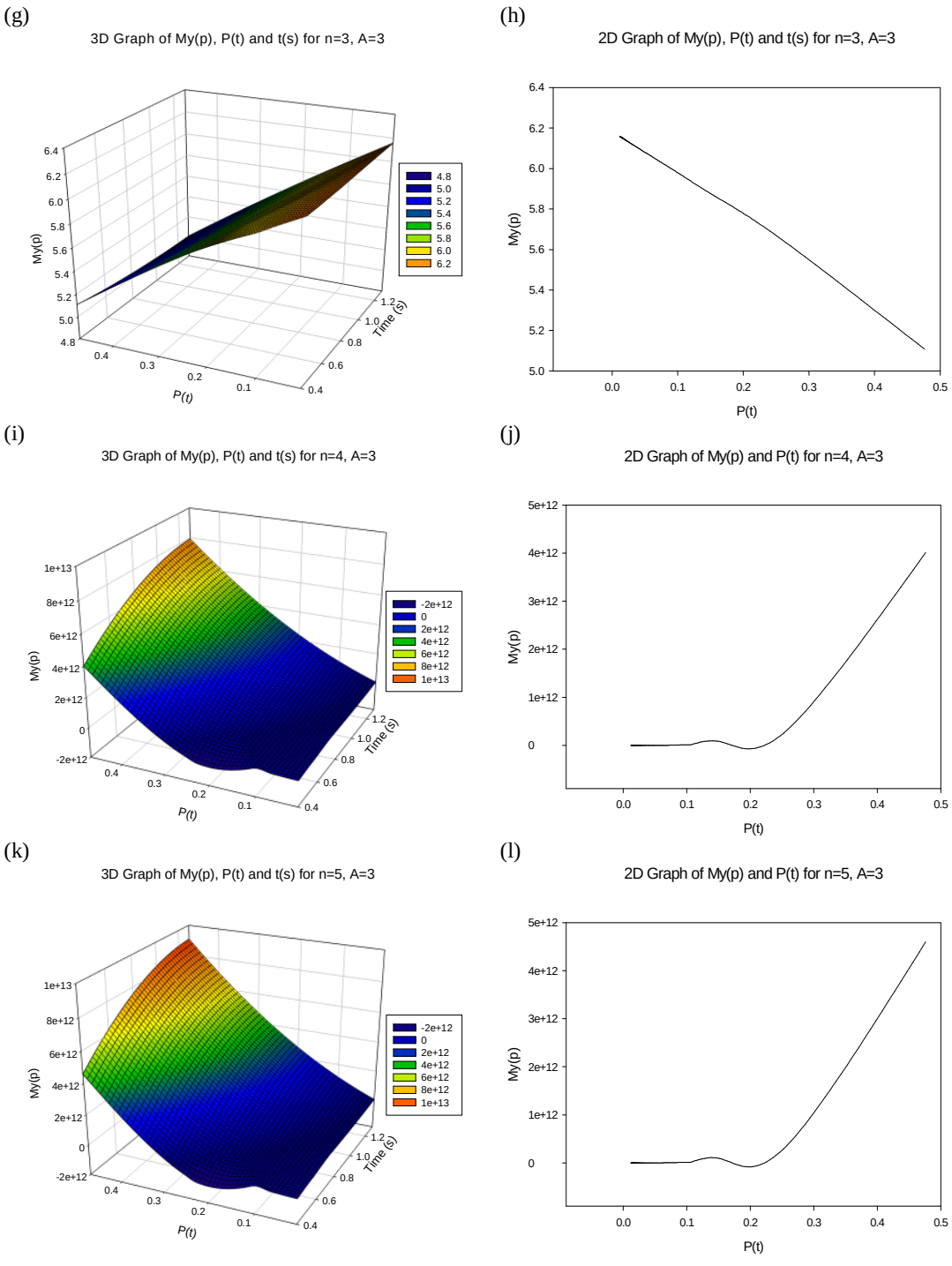

Fig. 15. 3D & 2D graph of equation (22) for A=3, Mo≠0, (a) n=0(b) n=0, (c) n=1, (d) n=1, (e) n=2, (f) n=2, (g) n=3, (h) n=3, (i) n=4, (j) n=4, (k) n=5, (l) n=5, for 3D and 2D respectively

(a)

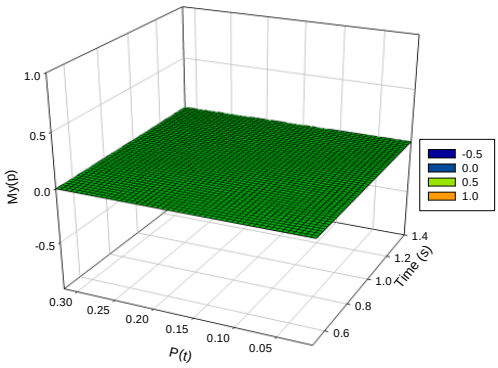
3D Graph of My(p), P(t) and t(s) for n=0, A=4
My(p)
P(t)
Time (s)
-0.5
0.0
0.5
1.0

(b)

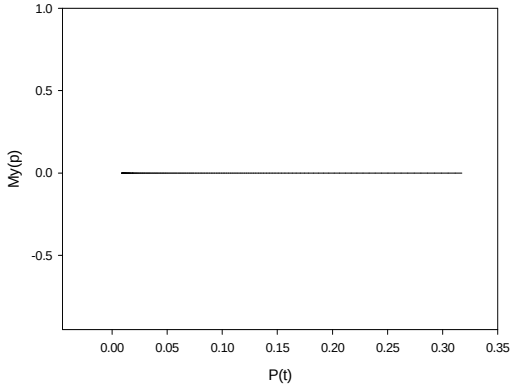
2D Graph of My(p) and P(t) for n=0, A=4
My(p)
P(t)

(c)

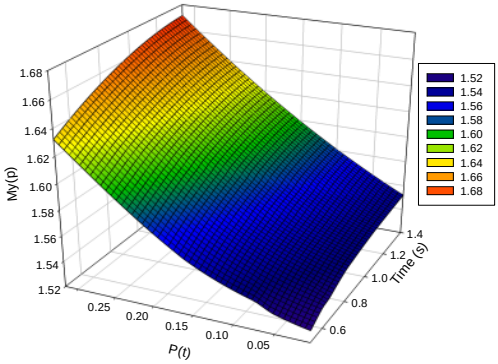
3D Graph of My(p), P(t) and t(s) for n=1, A=4
My(p)
P(t)
Time (s)
1.52
1.54
1.56
1.58
1.60
1.62
1.64
1.66
1.68

(d)

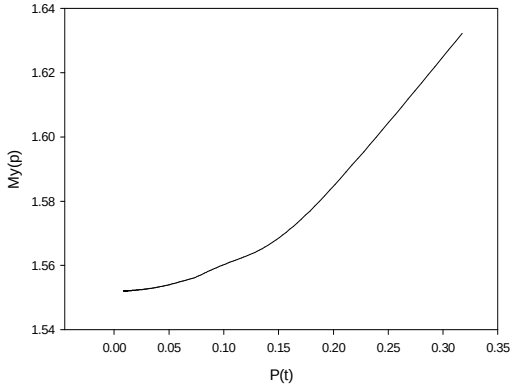
2D Graph of My(p) and P(t) for n=1, A=4
My(p)
P(t)

(e)

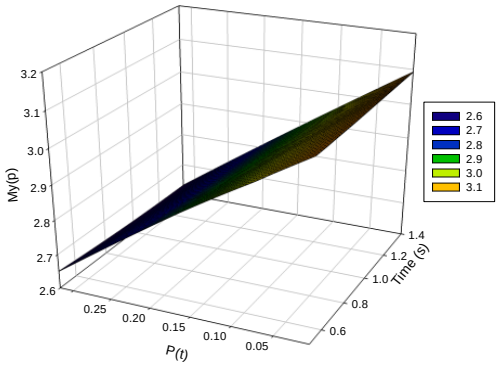
3D Graph of My(p), P(t) and t(s) for n=2, A=4
My(p)
P(t)
Time (s)
2.6
2.7
2.8
2.9
3.0
3.1

(f)

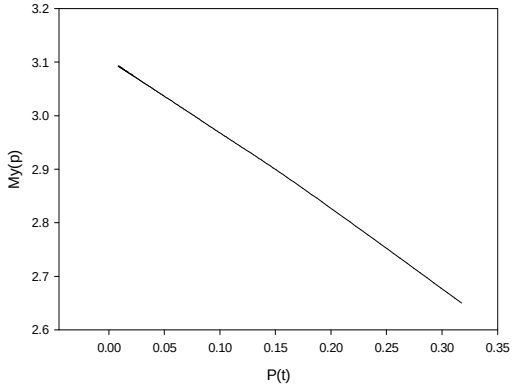
2D Graph of My(p) and P(t) for n=2, A=4
My(p)
P(t)

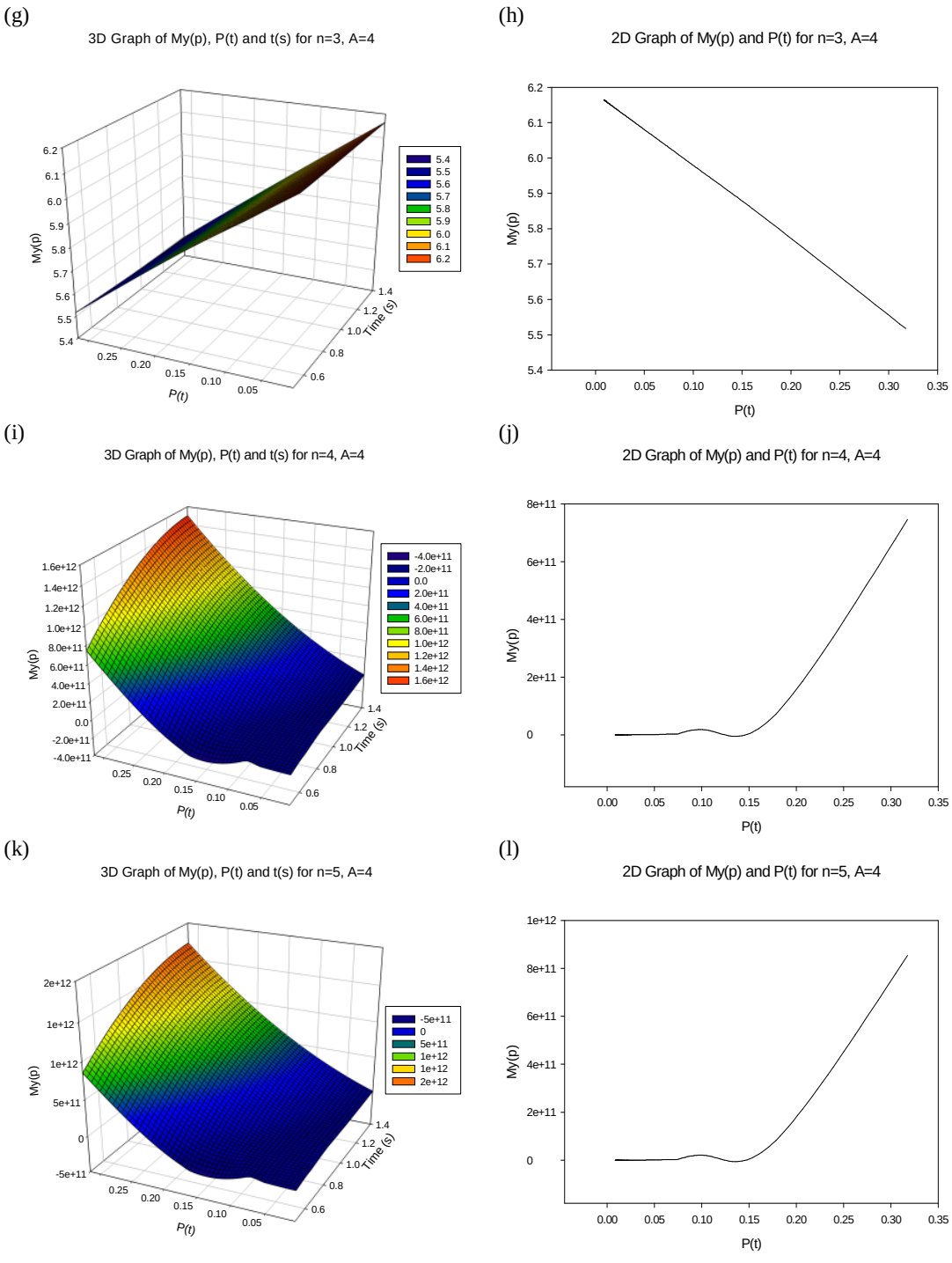

Fig. 16. 3D & 2D graph of equation (22) for A=4, Mo≠0, (a) n=0(b) n=0, (c) n=1, (d) n=1, (e) n=2, (f) n=2, (g) n=3, (h) n=3, (i) n=4, (j) n=4, (k) n=5, (l) n=5, for 3D and 2D respectively

(a)

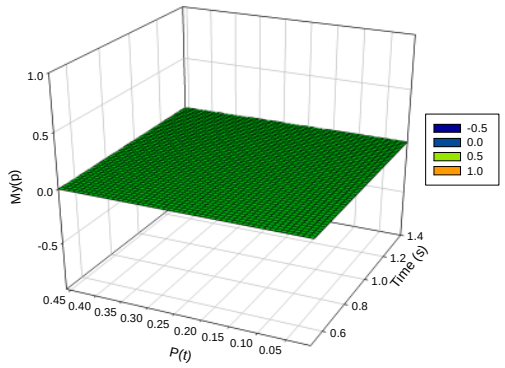
3D Graph of My(p), P(t) and t(s) for n=0, A=5
My(p)
P(t)
Time (s)
-0.5
0.0
0.5
1.0

(b)

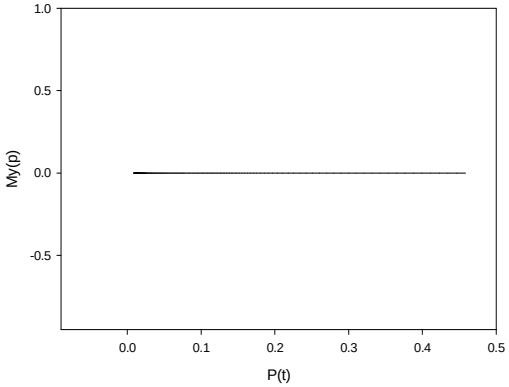
2D Graph of My(p) and P(t) for n=0, A=5
My(p)
P(t)

(c)

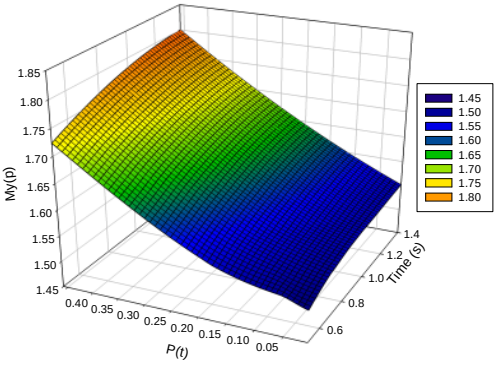
3D Graph of My(p), P(t) and t(s) for n=1, A=5
My(p)
P(t)
Time (s)
1.45
1.50
1.55
1.60
1.65
1.70
1.75
1.80

(d)

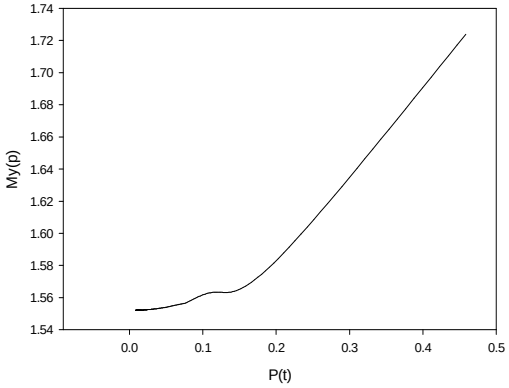
2D Graph of My(p) and P(t) for n=1, A=5
My(p)
P(t)

(e)

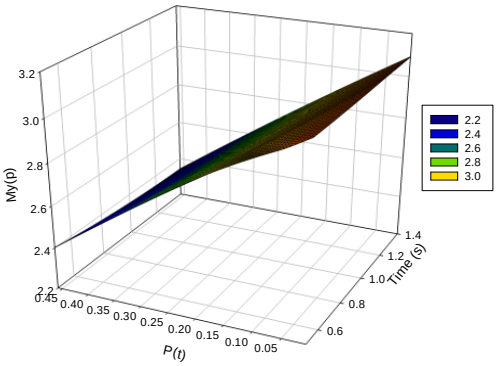
3D Graph of My(p), P(t) and t(s) for n=2, A=5
My(p)
P(t)
Time (s)
2.2
2.4
2.6
2.8
3.0

(f)

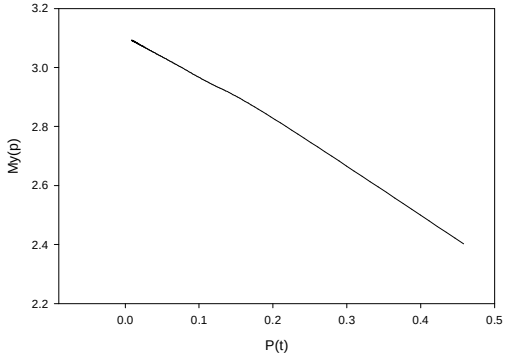
2D Graph of My(p) and P(t) for n=2, A=5
My(p)
P(t)

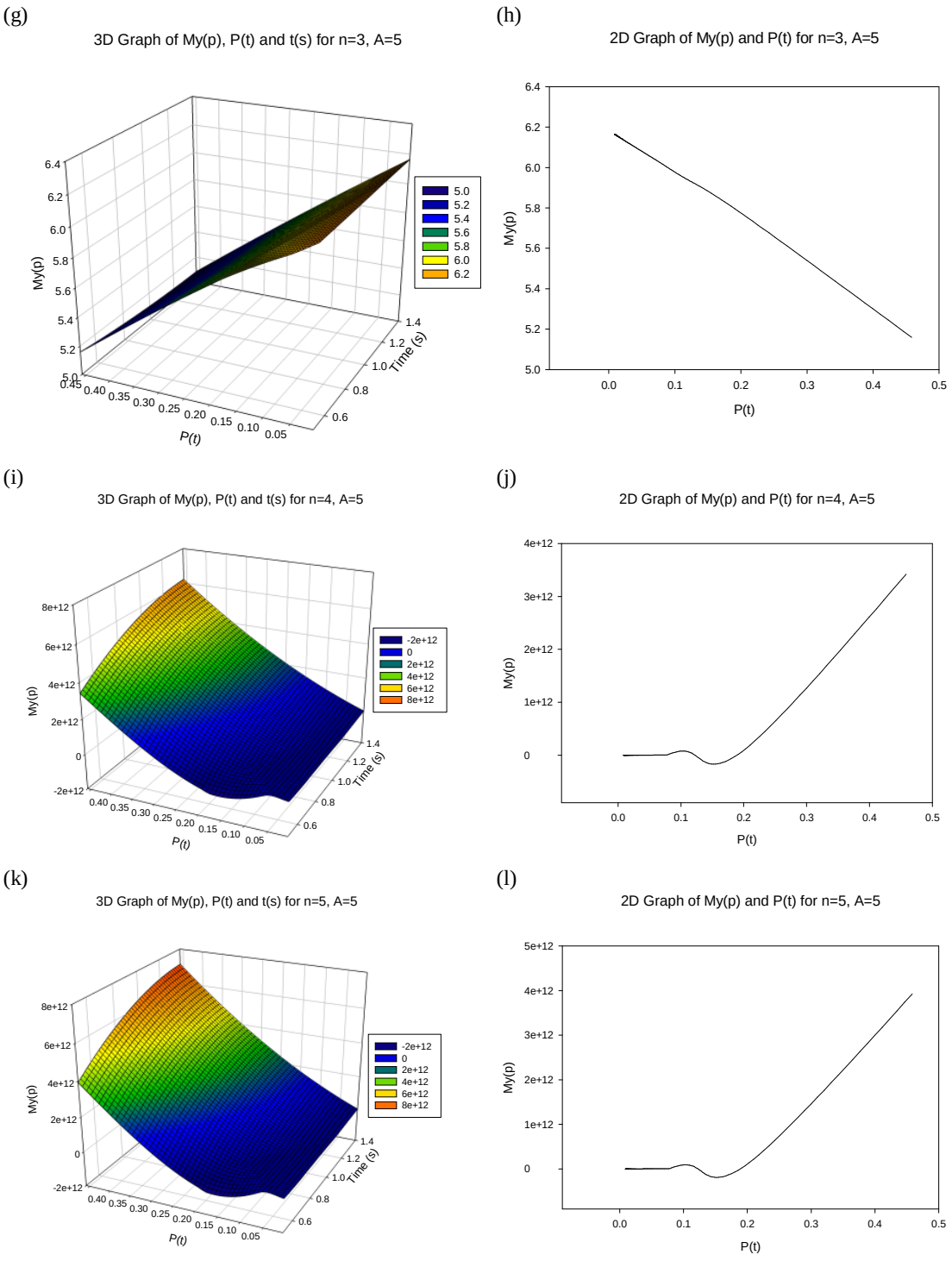

Fig. 17. 3D & 2D graph of equation () for A=5, Mo≠0, (a) n=0(b) n=0, (c) n=1, (d) n=1, (e) n=2, (f) n=2, (g) n=3, (h) n=3, (i) n=4, (j) n=4, (k) n=5, (l) n=5, for 3D and 2D respectively

7 Variation of p(t) with t(s) for Varying Values of 'A' and T_2

A transformation process in the quest to adapt the Bloch time dependent NMR equation (6) to a porous material gave rise to equation (11). The solution for a case where 'A' = 0 defined the porosity. Equation (11) was solved for a physical case when A is not equal to zero and a solution in equation (24) was obtained [3] to describe the influence of parameter A and spin-spin relaxation time (T_2) on porosity in porous media as shown in Fig. 18(a - h). The choice of T_2 relaxation time of 0.01 to 0.5 is typical of spin-spin relaxation time for blood flow.

It was observed that porosity become exponential for T_2 relaxation time =0.091 sec, while the constant A is varied from 1 to 5. A less significant full wave oscillation was also observed between time t=0.3 sec and 0.5 sec, as porosity increases, the time t for which porosity become measurable increases from 0.1 to 0.2 sec. This is a consequence of porosity becoming discontinuous at t=0 and 0.1 sec. Porosity again become more exponential for T_2 relaxation time = 0.172 sec while the constant A is varied from 1 to 5. A less significant oscillation was observed between time t=0.3 sec and 0.5 sec.

(a)

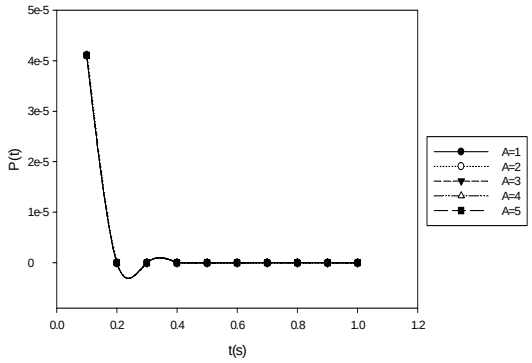

(b)

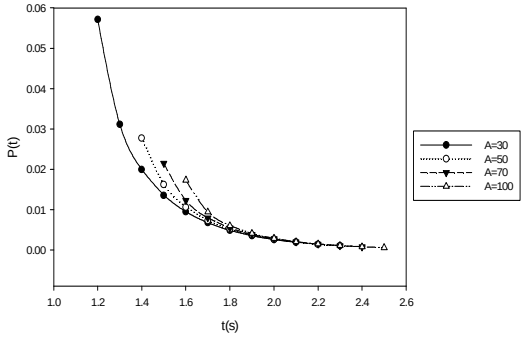

(c)

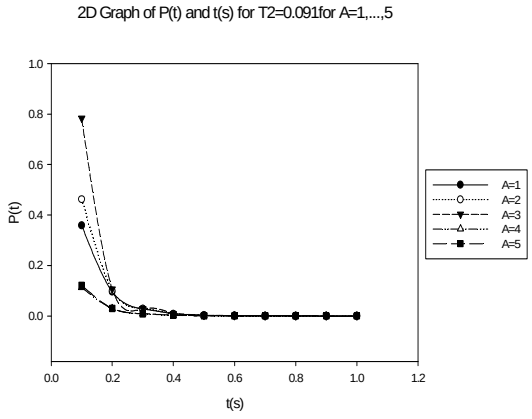

(d)

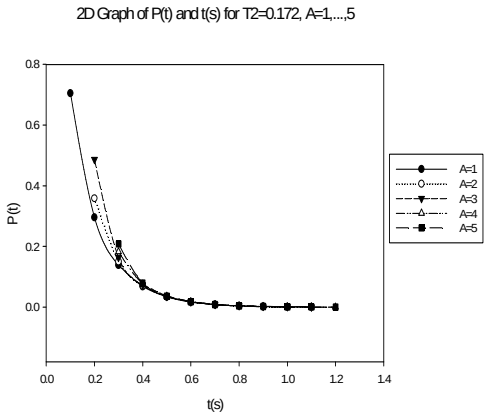

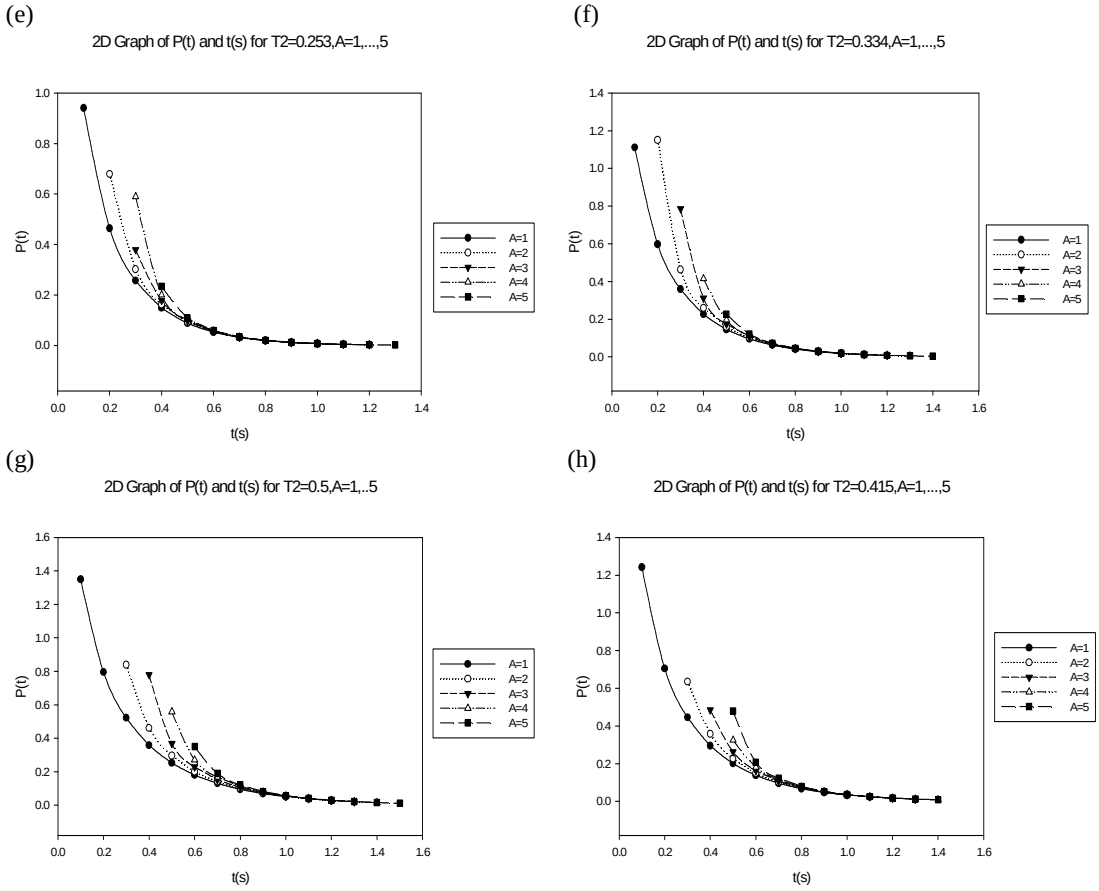

Fig. 18. Influence of parameter A and spin-spin relaxation time (T2) on porosity in porous media

8 Conclusion

We have presented analytical solution to time dependent Bloch equation for computational analysis of nano particles in porous media. Since the nano particle is expected to be imaged in a nano-porous medium (blood flow), we apply the transformation which make the transverse magnetization in time domain $M_y(t)$ measurable in the porous medium as $M_y(p)$ based on the condition that a^2 in equation (10) must be a positive integer and 'A' must be a constant. These conditions transforms $M_y(t)$ in a porous medium with porosity $p(t)$. The computational analyses of our results are also presented, which show the influence of parameter A on both the NMR transverse magnetization and the porosity P (t). The parameter 'A' and 'a' can give a lot of insight into other factors affecting the MR signal (M_y). We believe that with this solution in place, experts can now model bunch of parameters which a conventional fluid flow equation did not capture into the 'A' parameter, just like the exchange correlation functional in the density functional theory, which can then be evaluated numerically, through various approximation methods while optimizing the system. The results obtained in this study can have applications in functional magnetic resonance imaging (fMRI), Petroleum exploration and well design, geological engineering and could be a frontier towards a very robust way of describing porosity and permeability in systems transporting particles of specific shape and form.

The detailed possible application of this fundamental solution to explain and solve real life flow problems in which NMR -sensitive materials are transported through a small sized pore will be presented separately.

Acknowledgement

The Author is grateful to Dr. Yansun Yao of the Department of Physics and Engineering Physics, University of Saskatchewan, Canada. Also, to both Mr. Dada O.M, Prof. O. B Awojoyogbe of the department of Physics, Federal University of Technology, Minna and anonymous reviewers for their constructive comments. Finally, the author acknowledges the travel grant from AIMS under the POST-AIMS bursary programme which enabled the completion of this research work.

Competing Interests

Author has declared that no competing interests exist.

References

[1] Jaiswal BR, Gupta BR. Stokes flow over composite sphere: Liquid core with permeable shell. Journal of Applied Fluid Mechanics. 2015;8(3):339-350.

[2] Dada OM, Awojoyogbe OB, Ukoha AC. A computational analysis for quantitative evaluation of petrol-physical properties of rock fluids based on Bloch NMR diffusion model for porous media. Journal of Petroleum Science and Engineering. 2015;127:137-147.

[3] Adeleke AA. Analytical solution to fundamental Bloch NMR flow equations for non-zero porosity transformation parameter. International Journal of Theoretical and Mathematical Physics. 2016;6(2):86-91.
DOI: 10.5923/j.ijtmp.20160602.04

[4] Carrington Alan, Andrew D. McLachlan. Introduction to magnetic resonance: With applications to chemistry and chemical physics; 1969.

[5] Bogunia-Kubik K, Sugisaka M. From molecular biology to nanotechnology and nanomedicin. Biosystems. 2002;65(1):123.

[6] Desai TA, Chu WH, Tu JK, Beattie GM, Hayek A, Ferrari M. Biotechnol. Bioeng. 1998;57(1):118.

[7] Arthur G. Palmer. Relaxation and dynamic processes. Columbia University, USA; 1-14.

[8] Riegler J, Allain B, Cook RJ, Lythgoe MF, Pankhurt QA. Magnetically assisted delivery of cells using a magnetic resonsnce imaging system. 2010;1(1):1–5.

[9] Freitas Jr. RA. Nanomedicine. Basic capabilities. Landes Bioscience, Georgetown, TX. 1999;1(1):20-22.

[10] Arthurs Edison. Structural biology: Theory and applications of NMR spectroscopy, Class notes for BCH 6746. Spring, Florida, USA; 2000.

[11] Awojoyogbe OB. A mathematical model of the Bloch NMR equations for quantitative analysis of blood flow in blood vessels with changing cross section – I. Physica A. 2002;163-175.

[12] Awojoyogbe OB. A mathematical model of the Bloch NMR equations for quantitative analysis of blood flow in blood vessels with changing cross section – II. Physica A. 2003;534-550.

[13] Awojoyogbe OB, et al. Mathematical concept of the Bloch flow equations for general magnetic resonance imaging: A review. Concepts in Magnetic Resonance Part A. 2011;38(3):85-101.

[14] Awojoyogbe OB, Dada M, Faromika OP, Olufemi FM, Fuwape OP. Polynomial solutions of Bloch NMR flow equations for classical and quantum mechanical analysis of fluid flow in porous media. The Open Magnetic Resonance Journal. 2009;2(1):46-56.

[15] Storm, Arnold J, et al. Fast DNA translocation through a solid-state nanopore. Nano Letters. 2005;5(7):1193-1197.

[16] Freitas Jr. RA. Progress in nanomedicine and medical nanorobotics.
ISBN: 1-58883-042-X

[17] Freitas Jr. RA. Current status of nanomedicine and medical nanorobotics. Journal of Computational and Theoretical Nanoscience. 2005;2(1):1-25.

[18] Hamdi Mustapha, Antoine Ferreira. DNA nanorobotics. Handbook of Theoretical and Computational Nanotechnology. 2006;1(1):1-5.

[19] Juan Luis VazQuez. The porous medium equation (Mathematical Theory), Madrid; 1-7.

[20] Huihui Xu. Monitoring tissue engineering using magnetic resonance imaging. Journal of Biosecience and Bioengineering. 2008;106(6):515-527.

[21] Iserles A. A first course in numerical analysis of differential equation. Cambridge University Press, Cambridge. 1996;41-70.

Peer-review history:
The peer review history for this paper can be accessed here (Please copy paste the total link in your browser address bar)
http://sciencedomain.org/review-history/14872